

## Eightfold Shell Filling in a Double-Wall Carbon Nanotube Quantum Dot

Sunkyung Moon,<sup>1,2</sup> Woon Song,<sup>1</sup> Joon Sung Lee,<sup>1</sup> Nam Kim,<sup>1</sup> Jinhee Kim,<sup>1,\*</sup> Soon-Gul Lee,<sup>2</sup> and Mahn-Soo Choi<sup>3,†</sup>

<sup>1</sup>Korea Research Institute of Standards and Science, Daejeon 305-600, Korea

<sup>2</sup>Department of Applied Physics, Korea University, Chungnam 339-800, Korea

<sup>3</sup>Department of Physics, Korea University, Seoul 136-713, Korea

(Received 19 January 2007; published 25 October 2007)

We fabricated a quantum-dot device consisting of an individual double-wall carbon nanotube and studied its electrical transport properties at low temperatures. In the negative bias region, the gate modulation curve exhibited quasiperiodic current oscillations, attributed to the Coulomb blockade of single-electron tunneling. We observed both four- and eightfold shell filling in the Coulomb diamond structures. The observation implies an eightfold degeneracy in the single-particle energy levels, which is higher than the fourfold degeneracy of a single-wall carbon nanotube. We show that the observed eightfold shell filling is a unique characteristic of a double-wall carbon nanotube quantum-dot device.

DOI: [10.1103/PhysRevLett.99.176804](https://doi.org/10.1103/PhysRevLett.99.176804)

PACS numbers: 73.22.-f, 73.23.Hk, 73.63.Fg

A highly symmetric quantum mechanical system shows a rich structure of degenerate energy levels. A celebrated example is the shell structure of atoms and nuclei, whose states are characterized by radial and angular quantum numbers [1]. One can expect that a quantum dot (QD), also known as an artificial atom, exhibits a shell structure in the electronic energy levels when it has a proper degree of symmetry. Indeed, electronic shell filling has been observed in various types of symmetric QDs, such as metal clusters [2], small vertical semiconductor dots [3], and single-wall carbon nanotubes (SWNTs) [4,5].

Because the shell structure can be disrupted easily by breaking the relevant symmetry or overlapping in energy of the shells due to a large number of electrons, shell filling in a QD is difficult to observe. For example, the spectra of a nanoparticle [6], which is susceptible to the spatial imperfections and strong spin-orbit coupling, even lack the twofold spin degeneracy. Nanotube QDs are less influenced by spatial imperfection and clear shell filling is observed in a SWNT QD [4,5]. In an ideal SWNT QD, the orbital degeneracy along with the spin degeneracy leads to a fourfold shell filling in the single-electron energy levels [7,8]. Both two- and fourfold symmetries are observed in experiments. The less symmetric twofold degenerate structure (compared with the fourfold case) is attributed to the breaking of the orbital symmetry due to the electric contact.

A double-wall carbon nanotube (DWNT) consists of two concentric graphene sheets (so-called “walls”), interacting with each other via van der Waals’ force [9]. It is the simplest of multiwall carbon nanotubes (MWNTs). Unlike a SWNT, whose electron transport properties are relatively well understood, electron transport in a MWNT has long been controversial. At the center of the debates are the role of the interwall interaction and the relevance of interwall hopping [9–15]. Inner walls contribute to the electron transport by supplying an additional conduction channel and/or by modifying electronic properties of the

neighboring walls by interwall interaction. While several experiments indicate that the electric current is mainly carried by the outermost wall [10–13], theoretical studies suggest the importance of interwall hopping [14,15]. Electrons, injected from a metallic electrode to the outermost wall, may penetrate into the inner walls through quantum tunneling or thermal hopping. As the simplest form of MWNTs with only two walls, a DWNT is an ideal system to study the effects of the interwall interaction and the interwall coupling on electron transport. Further, MWNTs with more walls are usually more susceptible to defects (hence more diffusive) and their transport manifests less of the intrinsic symmetry of nanotubes. In this regard, the work by Buitelaar *et al.* [16] could be considered as a rare exception. To their own surprise, they observed the fourfold shell filling in a MWNT quantum dot.

In this Letter, we report an experimental study on the electrical transport through a DWNT QD. In the negative bias region, the DWNT QD exhibits clear Coulomb diamonds, in which we could identify both four- and eightfold patterns. The observed eightfold pattern suggests that the single-particle energy levels of the DWNT QD may have eightfold degeneracy in certain conditions. The proper experimental conditions for observing eightfold degenerate shell filling are reported below.

In our experiment, high-purity DWNTs were synthesized by catalytic decomposition of *n*-hexane over Fe-Mo/MgO catalyst. TEM study shows that more than 90% of the as-synthesized nanotubes were DWNTs. Less than 10% are SWNTs and triple-wall carbon nanotubes (TWNTs). TEM study and Raman analysis indicated that the diameters of DWNTs were in the range of 1.4 nm–2.5 nm and those of TWNTs were greater than 3 nm. We have dispersed synthesized carbon nanotubes in dichloroethane and spun over a highly doped Si substrate with a 300 nm-thick thermally grown SiO<sub>2</sub> layer.

Each nanotube was located by atomic force microscopy (AFM). In order to make our devices without a bundle of

SWNTs or an individual TWNT, we only chose nanotubes of diameter about 2 nm through AFM measurements. Figures 1(a) and 1(b) display an example of an AFM image. The lower part of the linear object in Fig. 1(a) has a height of about 2 nm [see curve A in Fig. 1(b)], and is considered to be a single strand of DWNT. On the other hand, the upper part of the linear object in Fig. 1(a) has the height of about 4 nm [curve B in Fig. 1(b)], and is a bundle of (most likely) DWNTs [17].

Once an individual DWNT was located by AFM, conventional electron-beam lithography was used to generate electrical lead patterns onto the selected DWNT. To form source and drain electrodes, magnetron sputtering at a base pressure of  $2 \times 10^{-7}$  Torr was used to deposit 40 nm of Co and 10 nm of Au, and a standard lift-off process is followed. The contact-to-contact distance was  $L \sim 250$  nm. Figure 1(c) shows a scanning electron microscopy image of a typical device. Electric transport properties were measured at the temperature of 2 K under vacuum. Conventional two-probe measurement was adopted and a back gate was used for gating. The two-probe resistance of the device was 16 k $\Omega$  at room temperature and 90 k $\Omega$  at the temperature of 2 K.

Figure 1(d) shows the gate modulation of the sample in the negative bias region. Quasiperiodic current oscillations are clearly seen. Observed quasiperiodic current oscillations are attributed to the Coulomb blockade of single-electron tunneling. We can distinguish more than 50 peaks in the measured range. Though we have not shown here, the full-range gate modulation curve exhibited  $n$ -channel dominant carbon nanotube field-effect transistor (CNFET) characteristics. Such results are interesting in that the most CNFET studied to date exhibit  $p$ -channel dominant characteristics, with rare exceptions [18–22]. The detailed mechanism for a CNFET conduction type is beyond the scope of this Letter [23]. The conduction gap in the gate

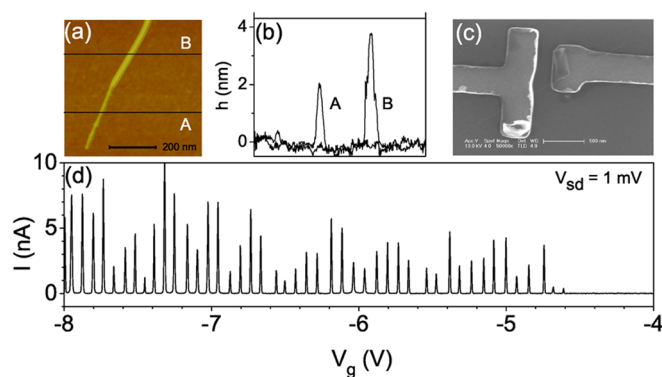


FIG. 1 (color online). (a) An atomic force microscopy image of a carbon nanotube. (b) Topography maps along the lines A and B in (a). (c) A scanning electron microscopy image of a typical device. (d) A gate modulation curve of the sample at 2 K with a source-drain bias of 1 mV.

modulation curve ( $V_g > -4.5$  V) indicates that the outer wall of the DWNT is semiconductive.

We have measured the differential conductance ( $dI/dV$ ) as a function of source-drain bias ( $V_{sd}$ ) and gate voltage ( $V_g$ ). A part of the data from a single-shot measurement is shown in Fig. 2. In Fig. 2, we observed several repeated symmetric patterns of Coulomb diamond structure. These symmetric Coulomb diamond patterns are the main focus of our Letter, and hereafter we discuss the physical implications of them in detail based on a simple model of DWNT.

The density plot of differential conductance (Fig. 2) reveals several noteworthy features: (i) The Coulomb diamond patterns are quasiperiodic. The periodicity is mostly fourfold, but notably eightfold in the gate voltage range from  $-6.3$  V to  $-5.6$  V. (ii) Each quasiperiodic pattern is bounded by distinctively larger diamonds, which we call *boundary diamonds* for later use. (iii) The borders of Coulomb diamond and the lines at higher bias voltages in each pattern look almost mirror symmetric with respect to the central diamond. To clarify such a mirror-symmetric feature, we have displayed highlighted image of the borders of Coulomb diamond and high-bias energy levels in Fig. 2(b) and 2(c). The dark lines denote mirror-symmetric borders while light lines represent asymmetric ones. A mirror-symmetric feature is apparent for the Coulomb diamond borders and also for most of high-order energy levels.

The mirror symmetry in the Coulomb diamond structure is typically related to the particle-hole symmetry and observed when nearly degenerate localized levels are occupied consecutively in the Coulomb blockade regime (the precise mirror symmetry is restored if the tunnel couplings of the degenerate levels to the leads are all equal) [24,25]. Therefore the observed Coulomb diamond structure in Fig. 2 strongly suggests an eightfold degeneracy in the

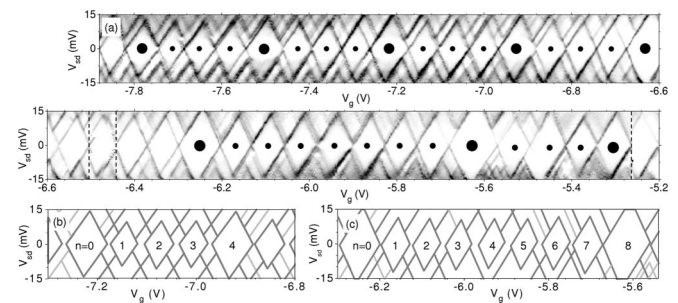


FIG. 2. (a) Density plot of the differential conductance ( $dI/dV$ ) as a function of the gate voltage  $V_g$  and source-drain bias voltage  $V_{sd}$ . The gate voltage range spans consecutive several fourfold shell-filling patterns and one eightfold pattern. The dashed lines indicate small jumps in the gate voltage. The small and large dots are a guide for eyes. (b) and (c) are highlighted images of the borders of the Coulomb diamond and the high-order energy levels. Dark lines denote mirror-symmetric ones while gray lines show asymmetric ones.

single-particle levels of the device in the gate voltage range from  $-6.3$  V to  $-5.2$  V, and a fourfold degeneracy in other gate voltage regions.

To the best of our knowledge, there has been no report of a carbon nanotube QD device showing eightfold mirror-symmetric Coulomb diamond structures. Most commonly observed is a twofold shell filling due to the spin degeneracy in the single-particle energy levels of SWNT. Theoretically, the unique orbital symmetry in SWNTs is expected to give a fourfold shell filling [26]. Indeed, such a fourfold shell filling has been demonstrated experimentally in SWNTs [7–9]. The even higher symmetric eightfold shell filling observed in our sample cannot be explained by the fourfold degeneracy from a single wall alone, but, rather, requires additional degeneracy. Below we will adopt a simple model of a DWNT and argue that our experimental observation can be explained by taking into account the linear (or parabolic) dispersion relation of each wall inherited from the graphene, a weak interwall coupling, and different gate coupling of the walls.

Before discussing the model, we estimate from Fig. 2 the single-electron charging energy  $U \equiv e^2/2C \sim 11.0$  meV, the single-particle level spacing  $\Delta \sim 3.5$  meV, and the level broadening  $\Gamma \sim 0.8$  meV. The single-electron charging energy is comparable to the theoretically estimated value  $C = (2\pi\epsilon_r\epsilon_0L)/\ln(2z/R)$ , where  $L \sim 250$  nm is the nanotube length and  $\epsilon_r \sim 4$  the dielectric constant of  $\text{SiO}_2$  and  $z \sim 300$  nm the thickness of  $\text{SiO}_2$  layer and  $R$  the radius of nanotube. It gives  $U \sim 9.4$  meV.

We first explore the implications of the electronic structure of each wall. A metallic SWNT of radius  $R$  and length  $L$  has single-particle energy levels,  $E_m = \hbar v_F k_m$ , where  $v_F \approx 8 \times 10^5$  m/s is the Fermi velocity and  $k_m$  is the quantized wave number in the longitudinal direction, given by  $\pi m/L$  ( $m = 1, 2, \dots$ ). The dispersion of a semiconducting SWNT is given by  $E_m = \hbar v_F \sqrt{k_m^2 + (1/3R)^2}$ . Assuming weak coupling between walls in DWNTs, the dispersion of each wall is still given as above.

If both walls of a DWNT are metallic, two walls have an identical set of quantized energy levels since their linear dispersion relations are independent of  $R$ . The electronic band of each wall has a fourfold degeneracy, two coming from orbital degeneracy and the other two from spin degeneracy, and overall ( $4 \times 2 = 8$ ) eightfold degeneracy is expected. Since all the energy levels are identical for the inner and outer wall, the eightfold symmetry should appear in the full range of gate voltage.

If both walls are semiconducting, then, due to the difference in diameters, there is a finite energy level mismatch  $\Delta E_m \equiv E_m^{\text{in}} - E_m^{\text{out}}$  between the single-particle energy levels,  $E_m^{\text{in}}$  and  $E_m^{\text{out}}$ , of the inner and outer wall, respectively. For  $3m\pi R \ll L$ ,  $\Delta E \approx \hbar v_F (R_{\text{in}}^{-1} - R_{\text{out}}^{-1})/3$ . With  $R_{\text{in}} = 0.66$  nm and  $R_{\text{out}} = 1.0$  nm in our sample,  $\Delta E \approx 91$  meV. Since the single-particle energy levels of the inner and outer wall are lifted relative to each other by a finite energy

difference  $\Delta E$ , which is several orders of magnitude larger than the level broadening ( $\Gamma \sim 0.8$  meV), only fourfold shell filling is expected. To the contrary, for  $3m\pi R \gg L$ ,  $\Delta E \approx 0$  and the inner and outer wall have matched energy levels. Thus more symmetric eightfold shell filling is expected. Similar results are obtained in the case where one wall is metallic and the other semiconducting.

The occurrence of a conduction gap in the gate modulation curve shown in Fig. 1(d) suggests that the outer wall should be semiconducting. According to the arguments above, fourfold shell filling is expected to occur near the band gap (small gate voltage) while eightfold shell filling is expected to occur deep inside the conduction or valence bands (large gate voltage) regardless of whether the inner wall is metallic or semiconducting. With  $L \sim 250$  nm and  $R \sim 1.0$  nm, we estimate that the necessary condition to observe an eightfold shell filling is  $m \gg 27$ . The eightfold shell filling was observed near  $V_g = -6.0$  V and the Coulomb blockade oscillations had the oscillation period  $\Delta V_g \sim 0.075$  V, as extracted from Fig. 2. With the Fermi energy  $E_F \approx -3.8$  eV estimated from the center of the conduction gap, we have  $m = (eV_g - E_F)/(e\Delta V_g) \approx 29$ .

According to the arguments above, however, eightfold shell filling is expected at all subsequent gate voltages, while in our sample eightfold shell filling was observed only once in the measured gate voltage range. This suggests that the single-particle energy levels of the inner and outer walls seldom match each other even in the deep conduction or valence band. To explain this, we take into account the effects of the different gate couplings of the inner and the outer walls. Since the inner wall is wrapped inside the outer wall and the electrical leads are contacted to the outer wall, the inner wall is coupled to the back gate via the outer wall. The screening by the outer wall naturally leads to weaker gate coupling for the inner wall than for the outer wall. The screening will be the most effective for metallic outer wall. However, even for a semiconducting outer wall, the screening cannot be ignored because of the large gate voltage (an effective hole doping) and the contacts to the electrodes [27].

For a more quantitative analysis, we define  $\alpha_{\text{in(out)}}$  to be the gate coupling constant of the inner (outer) wall, which determines the gate modulation  $\alpha_{\text{in(out)}}eV_g$  of the single-particle energy levels of the inner (outer) wall. The difference in the gate coupling makes the inner-wall levels lag behind the outer-wall levels by the amount  $\delta \equiv (\alpha_{\text{out}} - \alpha_{\text{in}})eV_g$  when  $\alpha_{\text{out}}eV_g$  spans one single-particle level spacing  $\Delta$ . If  $\delta \geq \Gamma$ , then eightfold shell filling will not be observed. As  $\alpha_{\text{out}}eV_g$  spans  $n\Delta$ , the energy levels of the inner-wall and the outer-wall levels will align again if the accumulated level mismatch,  $n\delta$ , becomes comparable to the single-particle level spacing ( $n\delta \approx \Delta$ ). Ideally, one should observe  $(2n - 3) \times 4$  Coulomb oscillation peaks between eightfold shell fillings. If we take  $\delta \approx \Gamma \approx 0.8$  meV and  $\Delta \approx 3.5$  meV, the value  $n \approx 4$  explains

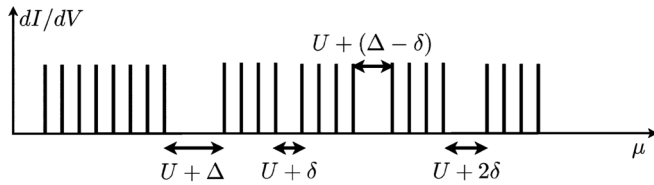


FIG. 3. A schematic of the conductance peaks pattern. Right after the eightfold shell-filling, the peak-to-peak spacing between two neighboring fourfold patterns will be given by  $U + \delta$ , which is much less than  $U + \Delta$ . The corresponding boundary Coulomb diamond thus becomes only slightly larger than those within a shell.

why we could observe the eightfold shell filling only once in the measured gate voltage range; more than 20 Coulomb diamonds are expected before and after an eightfold shell filling.

The level mismatch  $\delta$  can be extracted directly from  $dI/dV$  data in Fig. 2 as follows: The effect of the level mismatch  $\delta$  is most pronounced near the eightfold shell filling as demonstrated in Fig. 3. According to our model, the first two consecutive fourfold shell-filling patterns will be separated by  $U + \delta$ , which is much smaller than the usual value  $U + \Delta$  and which is only slightly larger than the value  $U$  within a shell. The corresponding boundary Coulomb diamond (the one at  $V_g = -5.3$  V in Fig. 2) thus becomes only slightly larger than those within the shell. In our data, such a small boundary Coulomb diamond is seen at  $V_g \approx -5.2$  V in Fig. 3. From Fig. 3, we thus estimate  $\delta \approx (2 \pm 1)$  meV, which is consistent with the estimation  $\delta \approx \Gamma \approx 0.8$  meV above.

In conclusion, we have observed both eightfold and fourfold shell fillings in a DWNT QD system. The fourfold degeneracy of the energy spectra of the constituent walls is a minimal requirement to explain our data. Our observation thus provides another experimental demonstration of the fourfold degeneracy of the graphene sheet in carbon nanotubes. Further, the eightfold shell filling requires weak but nonzero tunnel coupling between the inner and outer walls. Our result therefore confirms the possibility of electron tunneling into the inner walls at low temperatures.

The authors are grateful to C. J. Lee for providing high-purity DWNTs. This work was supported by the MOST through KOSEF. M.-S. C. was supported by the SRC/ERC Program (No. R11-2000-071), the KRF Grant (No. KRF-2005-070-C00055), and the Second BK21 Project.

\*jinhee@kriss.re.kr

†choims@korea.ac.kr

[1] E. P. Wigner, *Group Theory and Its Application to the Quantum Mechanics of Atomic Spectra* (Academic Press, New York, 1959).

- [2] W. D. Knight, K. Clemenger, W. A. de Heer, W. A. Saunders, M. Y. Chou, and M. L. Cohen, *Phys. Rev. Lett.* **52**, 2141 (1984).
- [3] S. Tarucha, D. G. Austing, T. Honda, R. J. van der Hage, and L. P. Kouwenhoven, *Phys. Rev. Lett.* **77**, 3613 (1996).
- [4] W. Liang, M. Bockrath, and H. Park, *Phys. Rev. Lett.* **88**, 126801 (2002).
- [5] D. H. Cobden and J. Nygard, *Phys. Rev. Lett.* **89**, 046803 (2002).
- [6] D. C. Ralph, C. T. Black, and M. Tinkham, *Phys. Rev. Lett.* **74**, 3241 (1995).
- [7] E. D. Minot, Y. Yaish, V. Sazonova, and P. L. McEuen, *Nature (London)* **428**, 536 (2004).
- [8] S. Zaric, G. N. Ostojic, J. Kono, J. Shaver, V. C. Moore, M. S. Strano, R. H. Hauge, R. E. Smalley, and X. Wei, *Science* **304**, 1129 (2004).
- [9] U. Coskun, T.-C. Wei, S. Vishveshwara, P. M. Goldbart, and A. Bezryadin, *Science* **304**, 1132 (2004).
- [10] S. Frank, P. Poncharal, Z. L. Wang, and W. A. deHeer, *Science* **280**, 1744 (1998).
- [11] A. Bachtold, C. Strunk, J.-P. Salvetat, J. Bonard, L. Forró, T. Nussbaumer, and C. Schönenberger, *Nature (London)* **397**, 673 (1999).
- [12] C. Schönenberger, A. Bachtold, C. Strunk, J.-P. Salvetat, and L. Forró, *Appl. Phys. A* **69**, 283 (1999).
- [13] J.-O. Lee, J.-R. Kim, J.-J. Kim, J. Kim, N. Kim, J. W. Park, K.-H. Yoo, and K.-H. Park, *Phys. Rev. B* **61**, R16362 (2000).
- [14] F. Triozon, S. Roche, A. Rubio, and D. Mayou, *Phys. Rev. B* **69**, 121410(R) (2004).
- [15] K.-H. Ahn, Y.-H. Kim, J. Wiersig, and K. J. Chang, *Phys. Rev. Lett.* **90**, 026601 (2003).
- [16] M. R. Buitelaar, A. Bachtold, T. Nussbaumer, M. Iqbal, and C. Schönenberger, *Phys. Rev. Lett.* **88**, 156801 (2002).
- [17] To be precise, the AFM topography (or the cross section measurement) alone is not enough to *completely* distinguish individual nanotubes from bundles.
- [18] M. Bockrath, J. Hone, A. Zettl, P. L. McEuen, A. G. Rinzier, and R. E. Smalley, *Phys. Rev. B* **61**, R10606 (2000).
- [19] V. Derycke, R. Martel, J. Appenzeller, and P. Avouris, *Appl. Phys. Lett.* **80**, 2773 (2002).
- [20] J. Kong, J. Cao, H. Dai, and E. Anderson, *Appl. Phys. Lett.* **80**, 73 (2002).
- [21] A. Javey, R. Tu, D. B. Farmer, J. Guo, R. G. Gordon, and H. Dai, *Nano Lett.* **5**, 345 (2005).
- [22] H. Oh, J.-J. Kim, W. Song, S. Moon, N. Kim, and J. Kim, *Appl. Phys. Lett.* **88**, 103503 (2006).
- [23] S. Moon, S.-G. Lee, W. Song, J. S. Lee, N. Kim, J. Kim, and N. Park, *Appl. Phys. Lett.* **90**, 092113 (2007).
- [24] Y. Meir, N. S. Wingreen, and P. A. Lee, *Phys. Rev. Lett.* **66**, 3048 (1991).
- [25] J. J. Palacios, L. Liu, and D. Yoshioka, *Phys. Rev. B* **55**, 15735 (1997).
- [26] H. Ajiki and T. Ando, *J. Phys. Soc. Jpn.* **62**, 1255 (1993).
- [27] V. Meunier, S. V. Kalinin, J. Shin, A. P. Baddorf, and R. J. Harrison, *Phys. Rev. Lett.* **93**, 246801 (2004).